FOREX Publication
Open Access | Rapid and quality publishing

International Journal of Electrical and Electronics Research (IJEER)
Research Article | Volume 13, Issue 4 | Pages 900-908 | e-ISSN: 2347-470X

Improving Frequency Response in a Microgrid Integrated with PV-HESS Using an FOPI Controller Optimized by the Grey Wolf Optimizer Algorithm

Thuy Duong Trinh[1], Van Hoan Hoang[2], Van Hung Nguyen[3*], The Thang Mai[4], and Trong Chuong Trinh[5]

[1]*Hanoi University of Industry, Hanoi, Vietnam; Email: trinhduonglhp@gmail.com*
[2]*Hanoi University of Industry, Hanoi, Vietnam; Email: vanhoan2423@gmail.com*
[3]*Hanoi University of Industry, Hanoi, Vietnam; Email: hung_nv@haui.edu.vn*
[4]*Hanoi University of Industry, Hanoi, Vietnam; Email: chuongtt@haui.edu.vn*
[5]*Hanoi University of Industry, Hanoi, Vietnam; Email: maithang@haui.edu.vn*

***Correspondence:** *Van Hung Nguyen, Email: hung_nv@haui.edu.vn; Tel.: +84 986 763 077*

ABSTRACT- The application of modern controllers for frequency regulation in standalone microgrids has been increasingly proven feasible. Among these, the Fractional Order Proportional-Integral (FOPI) controller with adjustable parameters has attracted considerable attention. The effectiveness of the FOPI controller is highly dependent on the proper tuning of its parameters. This paper proposes the use of the Grey Wolf Optimizer (GWO) algorithm to determine the optimal tuning parameters, with the objective of minimizing frequency oscillations. The simulation and performance evaluation are conducted using the MATLAB/Simulink platform. Additionally, comparisons are made with classical approaches including FOPI optimized by Particle Swarm Optimization (PSO), Genetic Algorithm (GA), standard FOPI, and conventional PI controllers, in order to assess the effectiveness of the proposed method.

Keywords: Frequency control, Microgrid (MG), PV, HESS, Fractional order PI (FOPI), Grey Wolf Optimizer (GWO), Particle Swarm Optimization (PSO).

ARTICLE INFORMATION

Author(s): Thuy Duong Trinh, Van Hoan Hoang, Van Hung Nguyen, The Thang Mai, and Trong Chuong Trinh;
Received: 16/04/2025; **Accepted:** 03/08/2025; **Published:** 30/12/2025;
E- ISSN: 2347-470X;
Paper Id: IJEER 1604-05;
Citation: 10.37391/ijeer.130430
Webpage-link:
https://ijeer.forexjournal.co.in/archive/volume-13/ijeer-130430.html

Publisher's Note: FOREX Publication stays neutral with regard to jurisdictional claims in Published maps and institutional affiliations.

1. INTRODUCTION

According to the International Energy Agency, by 2023, the global share of renewable energy had increased by nearly 50%, marking the fastest growth rate in the past two decades [1]. This indicates that renewable energy has been and continues to be strongly developed in many developed countries as well as worldwide. In particular, solar energy has been widely deployed and holds significant potential for sustainable energy production [2]. However, the intermittent nature of solar energy can adversely affect the stability and reliability of power systems. Consequently, the development of microgrids powered by solar energy is becoming an emerging trend. In order for a solar-integrated microgrid to operate in standalone mode, an energy storage system is essential for balancing power and maintaining grid stability [3]. Therefore, hybrid systems combining photovoltaic (PV) generation and battery energy storage systems (BESS) are considered a vital solution for microgrids that are characterized by uncertainty and sensitivity to environmental factors [4,5]. However, the specific characteristics of BESS, particularly regarding capacity and charge/discharge rate, may limit the system's dynamic response. To address this limitation, hybrid energy storage technologies integrating supercapacitors (SC) with BESS and PV systems have demonstrated enhanced performance. These systems offer both high storage capacity and fast charge-discharge capability, thereby improving the response time and ensuring better stability in standalone microgrids [6,7].

Alongside advancements in PV cell manufacturing and hybrid energy storage technologies, progress in control theory has led to the development of new control strategies aimed at improving system performance and enhancing coordination among components in microgrids. The PI controller has long been regarded as a core technology in control systems due to its simplicity in implementation and ease of parameter tuning. However, this conventional control method faces limitations in terms of response speed and adaptability, particularly when applied to systems with high uncertainty. PV energy systems, which are highly susceptible to environmental conditions such

FOREX Publication
Open Access | Rapid and quality publishing
International Journal of Electrical and Electronics Research (IJEER)
Research Article | Volume 13, Issue 4 | Pages 900-908 | e-ISSN: 2347-470X

as weather variations, represent a typical case where conventional PI control may prove inadequate. As a result, there is a growing need to improve traditional PI controllers by adopting alternative control techniques that offer faster response and better stability, thereby maximizing the operational potential of PV-HESS hybrid systems [8,9].

One approach to enhancing the performance of conventional PI controllers is the application of the fractional-order proportional-integral controller [10,11]. The FOPI controller integrates fractional calculus operators with conventional controller gains. The inclusion of a fractional-order integrator allows the FOPI controller to offer a broaders parameter tuning range compared to traditional PI controllers. This additional flexibility enables the FOPI controller to improve system stability, enhance transient response, and provide better noise rejection, particularly in systems characterized by nonlinear behavior and complex dynamics [12-14].

The use of FOPI controllers for improving frequency response in microgrids has been proposed in several studies [10,15]. However, these publications often lack a detailed explanation of the parameter selection and tuning process for FOPI controllers. This omission represents one of the main drawbacks of FOPI compared to other controllers. Parameter tuning for FOPI controllers is typically based on empirical adjustment methods or extensions of classical techniques such as the Ziegler–Nichols method. Therefore, determining the optimal parameters for FOPI controllers remains a significant challenge that hinders their widespread deployment in control systems.

Therefore, the Grey Wolf Optimizer algorithm is proposed to determine the optimal parameters of the FOPI controller in order to improve the frequency response speed of a microgrid integrated with PV-HESS. GWO is a nature-inspired optimization algorithm based on the hunting behavior of grey wolf packs [16]. It offers a good balance between exploration and exploitation in the search space, helping to avoid local optima and ensuring faster convergence compared to classical algorithms such as Particle Swarm Optimization and Genetic Algorithm (GA) [17-19]. The application of GWO for FOPI parameter optimization significantly improves the frequency deviation amplitude, shortens recovery time, and enhances the overall stability of the microgrid. Through simulation and control performance evaluation on a PV-HESS integrated microgrid modeled on the IEEE 6-bus test system, the effectiveness of the proposed approach is demonstrated in comparison with traditional methods for frequency regulation and microgrid stability enhancement. All simulations and evaluations are carried out using the MATLAB/Simulink platform.

2. STRUCTURE OF THE PV-HESS INTEGRATED MICROGRID

2.1. Modeling PV photovoltaic cells

A commonly used model for PV cells is the single-diode model, which represents the equivalent circuit of an ideal PV cell [20]. The equivalent electrical circuit of a practical PV cell is illustrated in *figure 1*.

In this model, R_s represents the series resistance, and R_{sh} denotes the shunt resistance. The value of R_{sh} is inversely proportional to the leakage current I_{sh} flowing through the shunt path.

The overall mathematical model of an ideal photovoltaic cell is expressed by the following equation [21]:

$$I = I_{PV} - I_O \left[exp\left(\frac{(N_S \times k \times T)V + R_S \times I}{q \times \alpha} \right) - 1 \right] - \frac{V + R_S \times I}{R_{sh}} \qquad (1)$$

The parameters of the PV cell include: I_{pv} is the current generated by solar irradiance, I_O is the diode saturation current, R_s and R_{sh} are the series and shunt resistances of the PV cell, α is the diode ideality factor. Other constants include: N_s is the number of series-connected cells, k is the Boltzmann constant (k = 1,3806503 × 10^{-23} JK^{-1}), T *is* the temperature of the diode (in Kelvin), and q is the electron charge (q = 1, 60217646 × $10^{-19}C$).

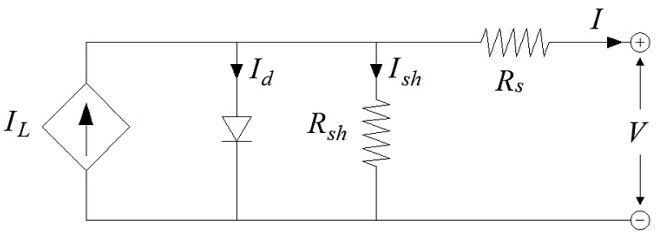

Figure 1. Mathematical Model of Photovoltaic Cell

2.2. Modeling Battery

The basic mathematical model of the battery energy storage system is shown in *figure 2*, consisting of resistive elements, capacitors, and a voltage source [22].

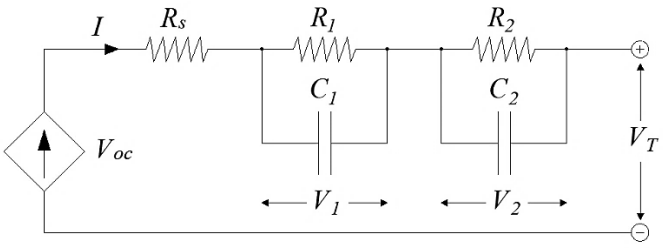

Figure 2. Mathematical Model of Battery Energy Storage System

By applying Kirchhoff's current law to the circuit, the following equations can be derived:

$$V_1'(t) = -\frac{1}{R_1 \times C_1} \times V_1(t) + \frac{I(t)}{C_1} \qquad (1)$$

$$V_2'(t) = -\frac{1}{R_2 \times C_2} \times V_2(t) + \frac{I(t)}{C_2} \qquad (2)$$

The voltage dynamics across V_1 and V_2 are expressed as $V_1'(t)$ and $V_2'(t)$, respectively.

FOREX Publication
Open Access | Rapid and quality publishing
International Journal of Electrical and Electronics Research (IJEER)
Research Article | Volume 13, Issue 4 | Pages 900-908 | e-ISSN: 2347-470X

By applying Kirchhoff's voltage law to the entire circuit, the total terminal voltage is given by:

$$V(t) = V_{OC}\big(Z(t)\big) - V_1(t) - V_2(t) - R_s \times I_t \quad (3)$$

Here, V_{OC} is the open-circuit voltage, and $V_1'(t)$, $V_2'(t)$ are the voltages across the parallel RC branches, while R_s is the internal resistance.

The state-space representation of the battery model is given in the general form:

$$X(t) = Ax(t) + Bu(t) \quad (4)$$
$$y(t) = Cx(t) + Du(t) \quad (5)$$

The state variable is defined as $x(t) = [V_1(t)\ V_2(t)]$, the input is $u(t) = I(t)$, the output is $y(t) = V_T(t)$, and the state-space matrices are defined as:

$$A = diag\left[-\frac{1}{R_1 \times C_1}\ -\frac{1}{R_2 \times C_2}\right] \quad (6)$$
$$B = \left[\frac{1}{C_1}\ \frac{1}{C_2}\right]^T \quad (7)$$
$$C = [-1\ -1] \quad (8)$$
$$D = [-R_s] \quad (9)$$

2.3. Modeling Supercapacitor

The mathematical model of a supercapacitor formed by capacitive and resistive elements is illustrated in *figure 3* [22], [23].

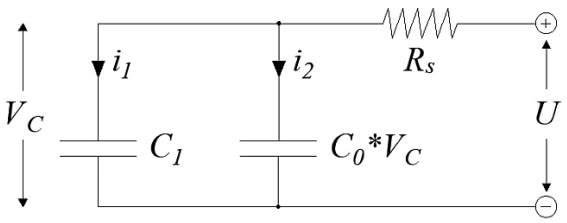

Figure 3. Mathematical Model of Supercapacitor

The terminal voltage U across the supercapacitor is expressed by the following equation:

$$U = i \times R_s + V_c \quad (10)$$

The total current through the supercapacitor can be written as:

$$i = i_1 + i_2 = C\frac{dVc}{dt} + C_0V_c\frac{dVc}{dt} \quad (11)$$

where, R_s is the internal resistance, and i_1, i_2 are the instantaneous currents through the equivalent capacitances C and C_0V_c.

Combining the equations, the state-space representation is simplified as:

$$\frac{dVc}{dt} = \frac{i}{C + C_0V_c} \quad (12)$$

2.4. Voltage Source Inverter

The frequency and voltage in a microgrid (MG) are maintained through the current control loop and the voltage control loop, in which the input signal for the current control loop is provided by the voltage control loop [24-26].

Figure 4 illustrates the input and output signals of the current and voltage control loops.

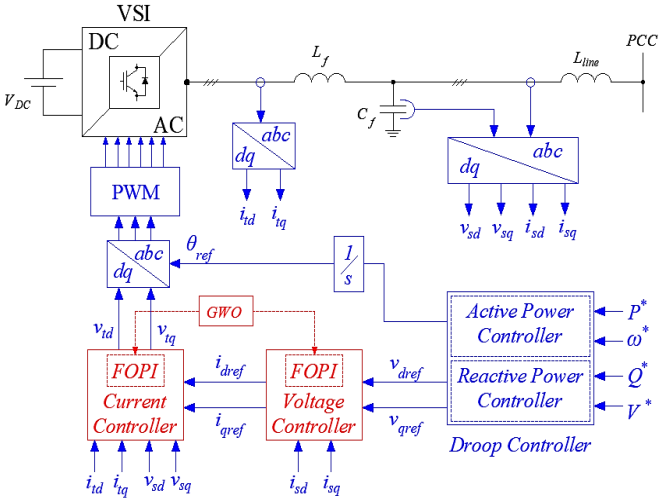

Figure 4. Structure and Control of VSI

Considering the state variable as the current on the inductive filter, the current control loop is expressed in the *dq* reference frame. With the input voltage vector, the current control equations are given by:

$$u_{di} = v_{td} + \omega Li_q - E_d \quad (13)$$
$$u_{qi} = v_{tq} - \omega Li_d - E_q \quad (14)$$

The current controller has the following transfer function:

$$G_c(s) = \frac{k_{pc} + k_{ic}s^{-\lambda}}{Ls + R + k_{pc} + k_{ic}s^{-\lambda}} \quad (15)$$

Given that the current response is significantly faster than that of the voltage loop, the current loop can be assumed to have reached steady state relative to the voltage loop [27,28]. Therefore, the current can be approximated as $i_d \approx i_{dref}$ and $i_q \approx i_{qref}$.

The voltage controller equations for the input signals are:

$$u_{de} = i_d - i_{Ld} + \omega CE_q \quad (16)$$
$$u_{qe} = i_q - i_{Lq} - \omega CE_d \quad (17)$$

The transfer function of the voltage controller is given by:

$$G_v(s) = \frac{k_{pv} + k_{iv}s^{-\lambda}}{C_s + k_{pv} + k_{iv}s^{-\lambda}} \quad (18)$$

FOREX Publication
Open Access | Rapid and quality publishing
International Journal of Electrical and Electronics Research (IJEER)
Research Article | Volume 13, Issue 4 | Pages 900-908 | e-ISSN: 2347-470X

3. OPTIMIZATION OF FOPI PARAMETERS USING THE GREY WOLF OPTIMIZER

3.1. Overview of the Grey Wolf Optimizer

In 2014, Mirjalili and colleagues proposed the GWO algorithm [29], inspired by the social hierarchy and natural hunting behavior of grey wolves. The dominance behavior of the alpha wolf determines the social ranking within the wolf pack. In GWO, the social hierarchy is divided into four organizational levels [30-32]:

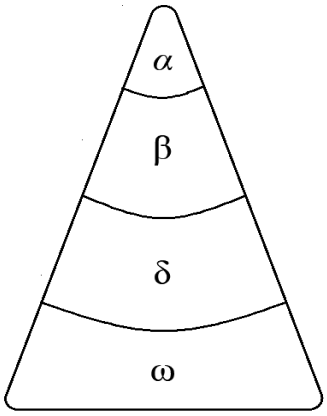

Figure 5. Social Hierarchical Structure of a Wolf Pack

The highest level in the social hierarchy is the alpha (α) wolves. Alphas are responsible for making decisions during the hunt, determining movement direction, and exercising overall leadership.

The second level of the hierarchy is occupied by beta (β) wolves, which support the alpha in decision-making and help enforce commands issued by the leader during hunting or pack movement.

The third level is represented by delta (δ) wolves, who are subordinate to both alpha and beta wolves. They monitor the lower-ranking wolves and enforce rules issued by the upper levels.

The lowest level consists of omega (ω) wolves. These wolves obey all orders and play no direct role in making decisions.

The hunting behavior of the top three wolves (α, β, δ) is used to simulate the exploitation phase of the GWO algorithm. Wolves typically surround prey, close in on it, and attack [32]. This behavior is mathematically modeled by the following equation:

$$F = \left|G.X_{prey}(t) - X(t)\right| \quad (19)$$

$$X(t+1) = X_{prey}(t) - D.F \quad (20)$$

Here, X_{prey} is the position of the prey, X is the current position of a wolf, t is the current iteration, and D, G are coefficient vectors calculated by:

$$D = 2.a.r_1 - a \quad (21)$$

$$G = 2.r_2 \quad (22)$$

In the above, r_1 và r_2 are random numbers uniformly distributed in the range (0, 1), and a is a control parameter that linearly decreases from 2 to 0 over the course of iterations. This mechanism allows GWO to transition from exploration to exploitation as the search progresses. The updated position of a wolf with respect to the alpha wolf can be expressed as:

$$X_1 = |X_\alpha - D_1.F_\alpha| \quad (23)$$

$$X_2 = \left|X_\beta - D_2.F_\beta\right| \quad (24)$$

$$X_3 = |X_\delta - D_3.F_\delta| \quad (25)$$

$$X(t+1) = \frac{X_1 + X_2 + X_3}{3} \quad (26)$$

In this context, X_α, $X_\beta$andX_δlần lượt là vị trí của alpha, beta và delta. represent the positions of the alpha, beta, and delta wolves, respectively. The exploration and exploitation behaviors of the search agents in GWO algorithm are governed by the parameter D. Specifically, the exploration phase occurs when $D \geq 1$, while the exploitation phase takes place when $D < 1$.

3.2. Objective Function for Fractional Order Proportional-Integral Parameter Optimization

A microgrid integrated with a PV-HESS hybrid energy system requires accurate frequency regulation, which plays a crucial role in determining the system's performance and dynamic stability. Therefore, the main objective of designing the FOPI controller is to ensure fast frequency response, robust control capability under disturbances, and improved dynamic behavior of the system. Selecting optimal values of K_p, K_i, and λ for the FOPI controller has a direct impact on the transient characteristics and response time of the controller, thereby enhancing the system's ability to suppress frequency deviations and maintain stability under load disturbances.

$$Min\ f(K_p, K_i, \lambda) = \omega_1.ITAE + \omega_2.\Delta f3_{settling_{max}} \quad (27)$$

Where,

ITAE (Integral of Time-weighted Absolute Error): A performance index that emphasizes the magnitude of error over time, aiming to minimize the area under the frequency deviation curve. It is defined as:

$$ITAE = \int_0^T t.\left|f_{ref} - f(t)\right|dt \quad (28)$$

Δf_{max}: The maximum frequency deviation from the reference during a disturbance. This value is critical in determining how well the controller suppresses large frequency deviations during transient events.

$t_{settling}$: The settling time, which indicates how fast the system returns to steady-state operation after a disturbance. Minimizing this time helps improve the dynamic response and recovery of the system.

FOREX Publication
Open Access | Rapid and quality publishing
International Journal of Electrical and Electronics Research (IJEER)
Research Article | Volume 13, Issue 4 | Pages 900-908 | e-ISSN: 2347-470X

The weighting factors ω_1, ω_2, ω_3 are chosen to reflect the relative importance of each performance index. In this study, the values are set as: $\omega_1 = 1$, $\omega_2 = 10$, and $\omega_3 = 5$, emphasizing the importance of limiting frequency overshoot while ensuring acceptable settling time and ITAE performance.

By minimizing the objective function, the GWO algorithm seeks the optimal set of FOPI controller parameters to enhance frequency regulation in the PV-HESS microgrid.

3.3. Implementation of Grey Wolf Optimizer for Fractional Order Proportional-Integral Parameter Turning

In this study, GWO is employed to optimize the parameters of the FOPI controller in order to improve the frequency response of a microgrid integrated with a hybrid PV-HESS energy source. The optimization is based on a selected objective function namely, ITAE which is a commonly used metric to assess the level of oscillation and the convergence speed of frequency response in microgrid systems. By applying the GWO algorithm, the controller is able to determine suitable parameter values that result in a fast and stable frequency response under various operating conditions.

During the optimization process, the grey wolf population is initialized with random values within the defined search bounds for the parameters K_P, K_I and λ. Each individual in the population represents a potential solution to the optimization problem and is evaluated using the microgrid system model implemented in the Simulink environment. The evaluation metrics include settling time, maximum overshoot, and the integral of time-weighted absolute error. The top three individuals in terms of performance are designated as α, β, and δ wolves. The remaining individuals ω adjust their positions according to the hunting strategy inspired by grey wolf behavior, in which their new positions are updated based on guidance from the three leading wolves. The algorithm's parameters are continuously updated to ensure a proper balance between exploration of the search space and exploitation of the best-found solutions [33,34].

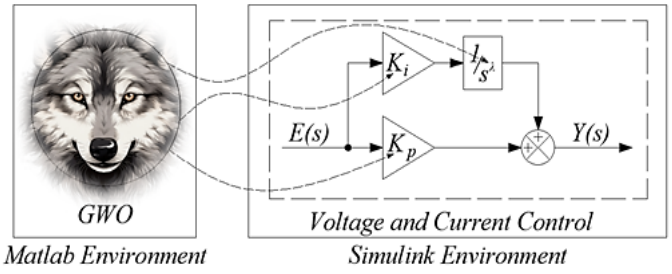

Figure 6. Optimization of the FOPI Controller Using Grey Wolf Optimizer

The overall operation of the grey wolf population follows the algorithmic flow illustrated in *figure 7*.

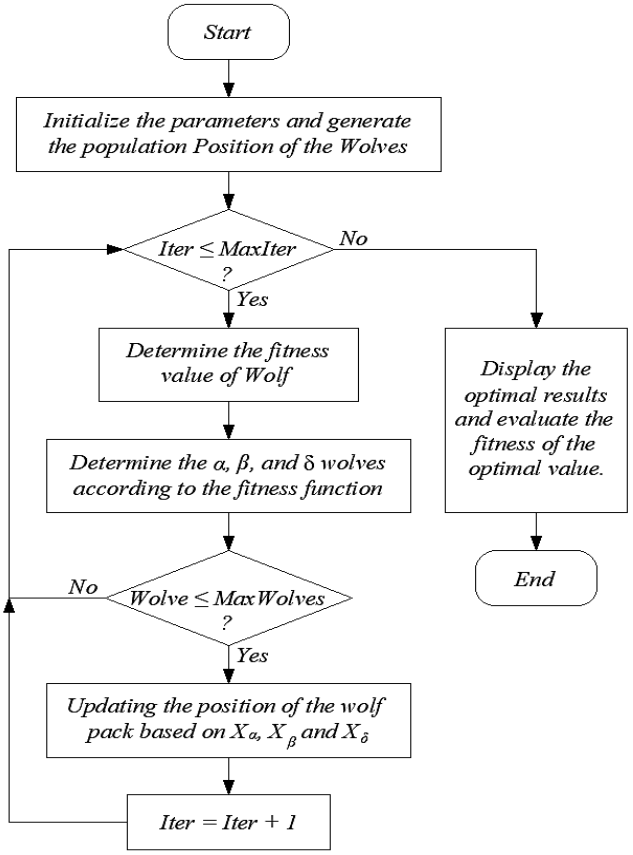

Figure 7. Flowchart of the Grey Wolf Optimizer Algorithm

The application of GWO for optimizing the FOPI controller in a microgrid system integrated with PV–HESS offers several advantages, including improved frequency response speed, reduced maximum overshoot, and enhanced overall control performance. Compared to other optimization methods such as PSO, GA, GWO demonstrates superior convergence capabilities and a lower risk of being trapped in local minima, thanks to its nature-inspired hunting mechanism.

4. SIMULATION AND RESULTS

The configuration of the simulated microgrid is depicted in *fig. 8*. The detailed specifications of the PV-BESS system are provided in *table 1*, while the line and load parameters are listed in *table 2*.

Table 3 presents the initial parameter constraints defined for the implementation of the GWO algorithm.

Table 1. PV-HESS system parameters

PV Array		SC	
Maximum Power	121275 W	Initial Voltage	540 V
Voltage at Maximum Power Point	300 V	Rate Capacitance	20 F
Current at Maximum Power Point	404.25 A	State of Charge	90%

FOREX Publication
Open Access | Rapid and quality publishing
International Journal of Electrical and Electronics Research (IJEER)
Research Article | Volume 13, Issue 4 | Pages 900-908 | e-ISSN: 2347-470X

BESS		Filter	
Nominal Voltage	500 V	Filter Resistance R_f	1.1 mΩ
Rate Capacity	1840 Ah	Filter Inductance L_f	0.35 mH
State of Charge	90%	Filter Capacitor C_f	0.44 mF
Cut-off Voltage	375 V		

Table 2. Line Impedance and load capacity

Line $Z_d = R_d + jX_d$ (pu), (S_b = 100 kVA; V_b = 0,38 kV)			
Line 1	0.20 + j0.25 pu	Line 5	0.20 + j0.25 pu
Line 2	0.05 + j 0.1 pu	Line 6	0.10 + j0.15 pu
Line 3	0.05 + j0.055 pu	Line 7	0.10 + j 0.15 pu
Line 4	0.10 + j0.15 pu		
$S = P + jQ$ (kVA)			
Load 2	73 + j20 kVA	Load 5	100 + j20 kVA
Load 3	50 + j20 kVA		

Table 3. Initial Parameter Constraints for the GWO Algorithm

Number of grey wolves	$N_{wolves} = 5$
Number of iterations	$N_{iterations} = 5$
Constraint on proportional gain	$0.001 \leq K_p \leq 100$
Constraint on integral gain	$0.001 \leq K_i \leq 50$
Constraint on fractional order of integrator	$0.001 \leq \lambda \leq 1$
Constraint on frequency deviation	$49.8 \leq f \leq 50.2$ Hz

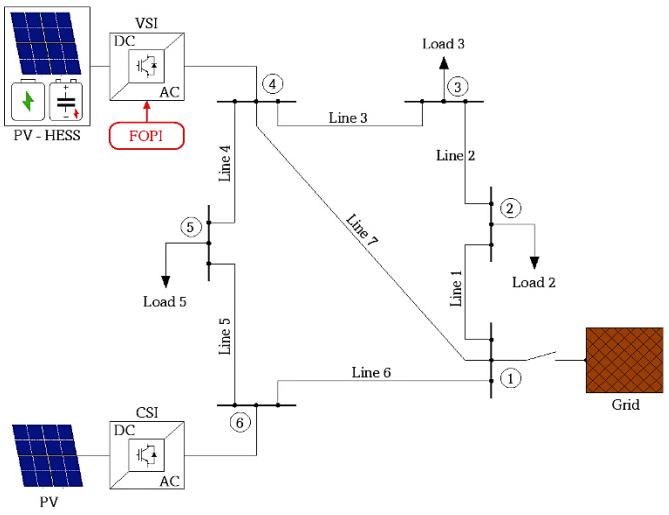

Figure 8. Autonomous Microgrid of 6-bus

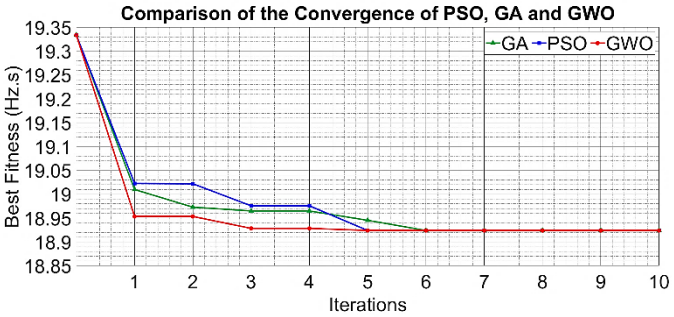

Figure 9. Comparison of the Convergence Characteristics of GWO, PSO, and GA

The effectiveness of the GWO in tuning the parameters of the FOPI controller to enhance frequency response in the PV-HESS system has been evaluated through a comparative analysis with two widely used optimization algorithms PSO and GA. As illustrated in *figure 9*, all three algorithms exhibit a downward convergence trend in the objective function value within the first five iterations. However, GWO demonstrates superior convergence characteristics, achieving the lowest best fitness value with a faster and more stable progression. Although both PSO and GA contribute to reducing the objective function value during the initial iterations, they tend to stagnate prematurely, indicating limited exploration capabilities and a higher tendency to be trapped in local optima. In contrast, GWO maintains continuous improvement over successive iterations without signs of stagnation, reflecting a well-balanced trade-off between exploration and exploitation throughout the search space. Notably, from the second iteration onward, GWO consistently outperforms PSO and GA by producing lower objective function values, thereby yielding higher-quality FOPI controller parameters. These findings validate the robustness and superior performance of the GWO algorithm in control parameter optimization, contributing significantly to enhanced frequency response and overall system stability in PV-HESS microgrid operations.

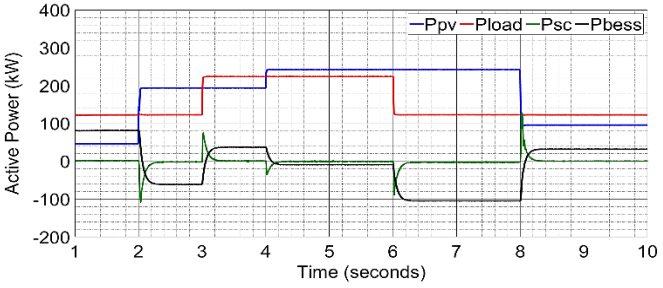

Figure 10. Power Flow Characteristic Curve in the Grid

To verify the real-time effectiveness of the optimized control strategy, a series of simulation scenarios were designed to assess the system's ability to maintain power balance in a PV-HESS integrated microgrid under varying operating conditions. The variation in active power during simulation is presented in *figure 10*, illustrating the flexible coordination between distributed energy sources. Specifically, the system is tested with changes in solar irradiance at time instances 2s and 7s, as well as load disturbances at 3s (increase) and 6s (decrease). The results

FOREX Publication
Open Access | Rapid and quality publishing
International Journal of Electrical and Electronics Research (IJEER)
Research Article | Volume 13, Issue 4 | Pages 900-908 | e-ISSN: 2347-470X

indicate that the system successfully maintains power balance and stable operation in the face of typical disturbances, thereby reinforcing the effectiveness of the GWO-optimized FOPI controller.

The primary objective of establishing the simulation scenarios is to comprehensively assess the effectiveness of the FOPI controller in regulating frequency response and ensuring system stability in the presence of active power fluctuations. The controller parameters are optimized using GWO, aiming to enhance dynamic performance under varying operating conditions. For benchmarking purposes, the proposed GWO-based method is systematically compared with alternative approaches, including PSO, GA, conventional parameter tuning techniques, and the traditional PI controller. This comparative analysis provides a robust basis for evaluating the relative performance and advantages of the proposed optimization strategy.

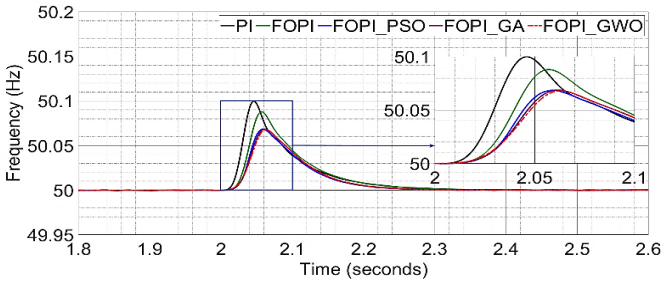

Figure 11. Frequency Characteristic Curve During Solar Irradiance Increase

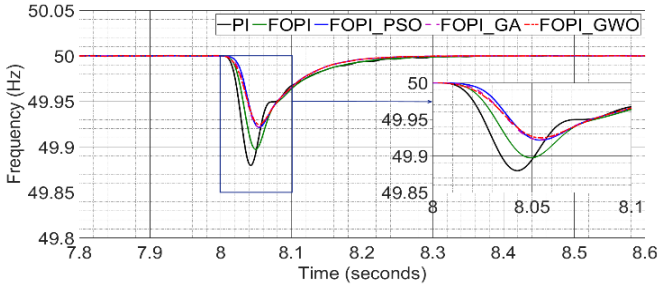

Figure 11. Frequency Characteristic Curve During Solar Radiation Reduction

Figures 11 and *12* present the simulation results of system frequency in order to demonstrate the regulation capability of the FOPI controller under varying solar irradiance conditions. Sudden changes in irradiance directly affect the power output of the PV system, resulting in frequency fluctuations within the microgrid. The FOPI controllers exhibit superior frequency regulation performance compared to the conventional PI controller. In particular, the GWO-optimized FOPI (FOPI_GWO) shows outstanding performance by significantly reducing frequency deviations and enabling faster recovery to steady-state conditions. Specifically, when solar irradiance increases abruptly, the PV output power rises, causing a power surplus and consequently a sharp frequency rise. Conversely, a sudden drop in irradiance leads to a reduction in PV power output, resulting in a power deficit and a corresponding frequency drop. In both scenarios, the PI controller produces the largest frequency deviations. The inclusion of the fractional-order integrator in the FOPI controller improves its damping characteristics, thereby reducing the amplitude of frequency oscillations. However, due to the use of non-optimized parameters, the standard FOPI controller does not achieve control performance comparable to that of the FOPI controllers optimized using PSO, GA, and GWO. These results confirm that proper parameter tuning plays a critical role in enhancing frequency control performance in PV-HESS-integrated microgrids.

Ensuring frequency stability during abrupt power load variations is a vital requirement for assessing control performance. In comparison to the traditional PI controller, the FOPI controller has much superior dynamic performance, especially in reducing the extent of frequency deviation during transient conditions. When optimized using metaheuristic algorithms like PSO, GA and GWO, the FOPI controller exhibits enhanced precision in frequency regulation and reactivity to load perturbations.

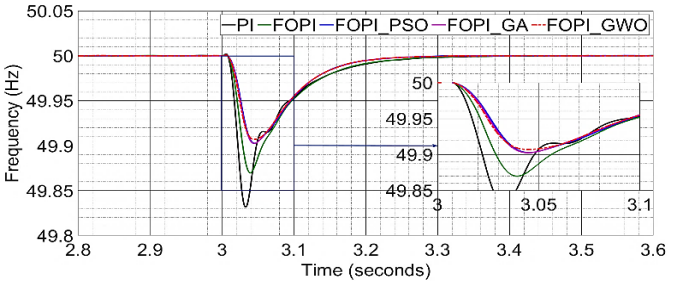

Figure 13. Frequency Response Curve During Load Power Increase

The control parameters optimized by the GWO method yield a lower frequency nadir and reduced settling time compared to those optimized by PSO, GA, demonstrating enhanced resistance to sudden load variations. Despite the little performance disparity between the two optimization techniques, the GWO-optimized FOPI controller regularly surpasses its alternative in terms of frequency deviation mitigation and convergence velocity during the control procedure. This result underscores the GWO algorithm's efficacy in comprehensively investigating the search space and circumventing local minima, therefore attaining more suitable controller settings for the system. *Figure 13* vividly illustrates these results, demonstrating the system's frequency response during a rapid load disturbance and confirming the higher performance of the GWO-based FOPI controller compared to alternative setups.

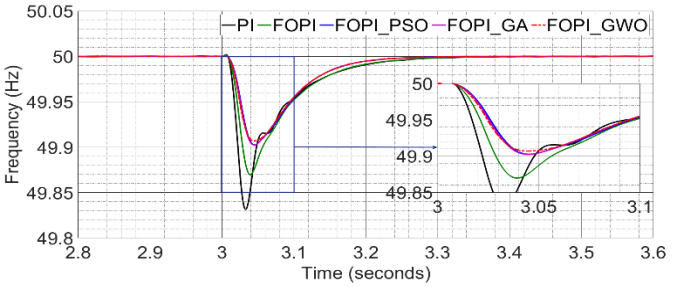

Figure 12. Frequency Response Curve during Load Shedding Event

FOREX Publication
Open Access | Rapid and quality publishing
International Journal of Electrical and Electronics Research (IJEER)
Research Article | Volume 13, Issue 4 | Pages 900-908|e-ISSN: 2347-470X

The capacity to sustain frequency stability during abrupt load-shedding events is a vital criterion for assessing the control quality in PV-HESS integrated microgrids. In such situations, sudden decreases in load demand can cause substantial frequency overshoot and extended oscillations if the control system is inadequately constructed. The traditional PI controller, due to its simplistic design and restricted tuning capabilities, exhibits insufficient responsiveness to load imbalance occurrences, leading to significant frequency deviations and prolonged settling periods, therefore undermining overall system stability.

The integration of a fractional-order integrator into the FOPI controller enhances flexibility in dynamic behaviour modulation, potentially leading to superior control performance. Nonetheless, without suitable parameter optimization, the FOPI controller continues to demonstrate significant frequency oscillations and sluggish convergence, highlighting the inadequacy of structural improvements alone in the absence of efficient parameter tuning methodologies.

Conversely, FOPI controllers optimized by metaheuristic algorithms like PSO, GA and GWO demonstrate markedly enhanced performance, efficiently mitigating frequency overshoot and enabling swifter recovery to the normal frequency. This enhancement is ascribed to the meticulous adjustment of control parameters, which augments the responsiveness and resilience of the controller amongst dynamic disturbances. The existence of a supplementary control loop enhances the system's capabilities for precise frequency regulation.

Figure 14 presents a comprehensive analysis and comparison of the system's frequency response during load-shedding conditions, underscoring the essential function of intelligent optimization algorithms in improving the dynamic attributes of frequency control strategies within PV-HESS microgrid settings.

5. CONCLUSIONS

This study proposed and evaluated the effectiveness of the FOPI controller in improving the frequency response of a microgrid integrated with a PV-HESS system. Compared to the conventional PI controller, the FOPI controller demonstrated superior control performance by reducing frequency deviations and maintaining system stability under load fluctuations and variable generation conditions. The effectiveness of the FOPI controller fundamentally depends on parameter selection, as the quality of these parameters directly influences the system's ability to mitigate oscillations and achieve faster recovery to steady-state frequency.

Therefore, the optimization of FOPI parameters is a critical component of the overall control strategy. Furthermore, the choice of optimization algorithm plays a vital role, as each algorithm has its own advantages and limitations. In this study, the GWO algorithm was employed to optimize the parameters of the FOPI controller with the objective of enhancing the control performance of the system. A detailed simulation model of the PV-HESS integrated microgrid was developed in the MATLAB/Simulink environment to evaluate the proposed approach.

The simulation results demonstrated that all three algorithms PSO, GA and GWO used to optimize the FOPI controller outperformed both the non-optimized FOPI and the conventional PI controller, particularly in reducing frequency oscillations and improving dynamic responsiveness. Analysis of the convergence behavior of the objective function revealed that GWO achieved a lower minimum value than both PSO and GA, owing to its hierarchical search mechanism based on the leadership structure of alpha, beta, and delta wolves, which enables enhanced exploration of the solution space. In contrast, PSO and GA rely on inertia and population-based evolutionary mechanisms, which increases the likelihood of premature convergence to local optima. These findings confirm that the GWO algorithm offers a more effective and flexible approach for optimizing FOPI controller parameters, thereby improving frequency regulation and operational stability in microgrids operating under dynamic and unpredictable conditions.

Author Contributions: The fundamental execution of this study, encompassing the creation of the simulation model, implementation of optimization algorithms, and preliminary data analysis, was conducted by Thuy Duong Trinh and Van Hoan Hoang. Van Hung Nguyen was instrumental in developing the methodological framework, significantly aiding in the formulation of the control strategy, enhancement of the simulation architecture, and validation of the outcomes. He offered comprehensive technical feedback during the drafting process and played a crucial role in the manuscript's revision and improvement. Thang Mai and Trong Chuong Trinh provided conceptual direction for the research, offering strategic guidance, reviewing interim findings, and aiding in the critical assessment of the manuscript before submission. All authors have reviewed and consented to the published version of the manuscript.

Acknowledgments: The authors also appreciate the assistance and valuable discussions provided by colleagues and research collaborators during the preparation of this manuscript.

Funding: This research received no external funding.

Conflicts of Interest: The authors declare no conflict of interest.

REFERENCES

[1] International Energy Agency, "Renewables 2020," *Paris*. 2020. doi: 10.1002/peng.20026.

[2] I. T. Force *et al.*, "Trends in Microgrid Control," vol. 5, no. 4. pp. 1905–1919, 2014.

[3] P. Patel, "Modeling , Stability Analysis and Control of Renewable Driven Islanded and Grid Connected Microgrids," no. June. 2011.

[4] M. I. Juma, B. M. M. Mwinyiwiwa, C. J. Msigwa, and A. T. Mushi, "Design of a hybrid energy system with energy storage for standalone DC microgrid application," *Energies*, vol. 14, no. 18. MDPI, Sep. 2021. doi: 10.3390/en14185994.

[5] N. Vazquez, S. S. Yu, T. K. Chau, T. Fernando, and H. H. C. Iu, "A Fully Decentralized Adaptive Droop Optimization Strategy for Power Loss Minimization in Microgrids with PV-BESS," *IEEE Transactions on Energy Conversion*, vol. 34, no. 1. pp. 385–395, 2019. doi: 10.1109/TEC.2018.2878246.

[6] A. Almousawi and A. Aldair, "Control Strategy for a PV-BESS-SC Hybrid System in Islanded Microgrid," *Iraqi Journal for Electrical and Electronic Engineering*, vol. 19, no. 1. College of Engineering, University of Basrah, pp. 1–11, Jun. 2023. doi: 10.37917/ijeee.19.1.1.

[7] S. Kotra and M. K. Mishra, "A Supervisory Power Management System for a Hybrid Microgrid With HESS," *IEEE Transactions on Industrial*

Electronics, vol. 64, no. 5. pp. 3640–3649, May 2017. doi: 10.1109/TIE.2017.2652345.

[8] M. U. Mutarraf, Y. Terriche, K. A. K. Niazi, F. Khan, J. C. Vasquez, and J. M. Guerrero, "Control of hybrid diesel/PV/battery/ultra-capacitor systems for future shipboard microgrids," *Energies*, vol. 12, no. 18. MDPI AG, Sep. 2019.

[9] S. Wen, S. Wang, G. Liu, and R. Liu, "Energy Management and Coordinated Control Strategy of PV/HESS AC Microgrid During Islanded Operation," *IEEE Access*, vol. 7. pp. 4432–4441, 2019.

[10] S. H. Sikder, M. M. Rahman, S. K. Sarkar, and S. K. Das, "Fractional order robust PID controller design for voltage control of islanded microgrid," *4th International Conference on Electrical Engineering and Information and Communication Technology, iCEEiCT 2018*, no. August. pp. 234–239, 2018. doi: 10.1109/CEEICT.2018.8628040.

[11] D. Pullaguram, S. Mishra, N. Senroy, and M. Mukherjee, "Design and Tuning of Robust Fractional Order Controller for Autonomous Microgrid VSC System," *IEEE Transactions on Industry Applications*, vol. 54, no. 1. pp. 91–101, Jan. 2018. doi: 10.1109/TIA.2017.2758755.

[12] M. F. Mahmoud, A. T. Mohamed, R. A. Swief, L. A. Said, and A. G. Radwan, "Arithmetic optimization approach for parameters identification of different PV diode models with FOPI-MPPT," *Ain Shams Engineering Journal*, vol. 13, no. 3. Faculty of Engineering, Ain Shams University, p. 101612, 2022. doi: 10.1016/j.asej.2021.10.007.

[13] H. S. Ramadan, "Optimal fractional order PI control applicability for enhanced dynamic behavior of on-grid solar PV systems," *International Journal of Hydrogen Energy*, vol. 42, no. 7. Elsevier Ltd, pp. 4017–4031, 2017. doi: 10.1016/j.ijhydene.2017.01.122.

[14] M. M. Mahmoud *et al.*, "Application of Whale Optimization Algorithm Based FOPI Controllers for STATCOM and UPQC to Mitigate Harmonics and Voltage Instability in Modern Distribution Power Grids," *Axioms*, vol. 12, no. 5. 2023. doi: 10.3390/axioms12050420.

[15] H. A. Abumeteir and A. M. Vural, "Design and Optimization of Fractional Order PID Controller to Enhance Energy Storage System Contribution for Damping Low-Frequency Oscillation in Power Systems Integrated with High Penetration of Renewable Sources," *Sustainability (Switzerland)*, vol. 14, no. 9. 2022. doi: 10.3390/su14095095.

[16] M. A. Hasan, A. A. Oglah, and M. J. Marie, "Optimal FOPI-FOPD controller design for rotary inverted pendulum system using grey wolves' optimization technique," *Telkomnika (Telecommunication Computing Electronics and Control)*, vol. 21, no. 3. pp. 657–666, 2023. doi: 10.12928/TELKOMNIKA.v21i3.24383.

[17] D. Murugesan, K. Jagatheesan, P. Shah, and R. Sekhar, "Fractional order PIλDμ controller for microgrid power system using cohort intelligence optimization," *Results in Control and Optimization*, vol. 11, no. October 2022. Elsevier B.V., p. 100218, 2023. doi: 10.1016/j.rico.2023.100218.

[18] M. F. Cells, "Optimization / Genetic Algorithm (PSO / GA) in a DC / DC Converter for Improving the Performance of Proton-Exchange." 2024.

[19] R. Rajesh, "Optimal tuning of FOPID controller based on PSO algorithm with reference model for a single conical tank system," *SN Applied Sciences*, vol. 1, no. 7. Springer International Publishing, pp. 1–14, 2019. doi: 10.1007/s42452-019-0754-3.

[20] T. B. Seane, R. Samikannu, and T. Bader, "A review of modeling and simulation tools for microgrids based on solar photovoltaics," *Frontiers in Energy Research*, vol. 10, no. September. pp. 1–20, 2022. doi: 10.3389/fenrg.2022.772561.

[21] O. Abdelkhalek *et al.*, "Modeling and Control a DC-Microgrid Based on PV and HESS Hybrid Energy Storage System," no. April. 2019. [Online]. Available: https://www.researchgate.net/publication/333774379

[22] S. K. Ramu, I. Vairavasundaram, B. Aljafari, and T. Kareri, "Design of PV, Battery, and Supercapacitor-Based Bidirectional DC-DC Converter Using Fuzzy Logic Controller for HESS in DC Microgrid," *Journal of Electrical and Computer Engineering*, vol. 2024. 2024. doi: 10.1155/2024/3035524.

[23] J. Zeng, B. Zhang, C. Mao, and Y. Wang, "Use of battery energy storage system to improve the power quality and stability of wind farms," *2006 International Conference on Power System Technology, POWERCON2006*. pp. 1–6, 2006. doi: 10.1109/ICPST.2006.321662.

[24] Y. Li and L. Fan, "Stability Analysis of Two Parallel Converters with Voltage-Current Droop Control," *IEEE Transactions on Power Delivery*, vol. 32, no. 6. pp. 2389–2397, 2017. doi: 10.1109/TPWRD.2017.2656062.

[25] D. B. Rathnayake *et al.*, "Grid Forming Inverter Modeling, Control, and Applications," *IEEE Access*, vol. 9. IEEE, pp. 114781–114807, 2021. doi: 10.1109/ACCESS.2021.3104617.

[26] A. Yazdani and R. Iravani, "A unified dynamic model and control for the voltage-sourced converter under unbalanced grid conditions," *IEEE Trans. Power Deliv.*, vol. 21, no. 3, pp. 1620–1629, 2006.

[27] J. Belikov and Y. Levron, "A Sparse Minimal-Order Dynamic Model of Power Networks Based on dq0 Signals," vol. 8950, no. c. pp. 1–9, 2017. doi: 10.1109/TPWRS.2017.2702746.

[28] R. Yazdani, A., & Iravani, "Voltage-sourced converters in power systems: Modeling, control, and applications," pp. 211–217, 2010.

[29] S. Mirjalili, S. M. Mirjalili, and A. Lewis, "Grey Wolf Optimizer," *Advances in Engineering Software*, vol. 69. Elsevier Ltd, pp. 46–61, 2014. doi: 10.1016/j.advengsoft.2013.12.007.

[30] J. Agarwal, G. Parmar, R. Gupta, and A. Sikander, "Analysis of grey wolf optimizer based fractional order PID controller in speed control of DC motor," *Microsystem Technologies*, vol. 24, no. 12. pp. 4997–5006, 2018. doi: 10.1007/s00542-018-3920-4.

[31] U. B. Tayab, J. Lu, S. Taghizadeh, A. S. M. Metwally, and M. Kashif, "Microgrid energy management system for residential microgrid using an ensemble forecasting strategy and grey wolf optimization," *Energies*, vol. 14, no. 24. pp. 1–19, 2021. doi: 10.3390/en14248489.

[32] S. K. Verma and R. Devarapalli, "Fractional order PIλDμ controller with optimal parameters using Modified Grey Wolf Optimizer for AVR system," *Archives of Control Sciences*, vol. 32, no. 2. pp. 429–450, 2022. doi: 10.24425/acs.2022.141719.

[33] J. Zhang, X. Wang, and L. Ma, "An optimal power allocation scheme of microgrid using grey wolf optimizer," *IEEE Access*, vol. 7. pp. 137608–137619, 2019. doi: 10.1109/ACCESS.2019.2942352.

[34] B. S. Goud *et al.*, "PV/WT Integrated System Using the Gray Wolf Optimization Technique for Power Quality Improvement," *Frontiers in Energy Research*, vol. 10, no. August. pp. 1–14, 2022. doi: 10.3389/fenrg.2022.957971.